



Protective Action of SIRT1 Activator Aptamer in Human Skin Cell Line

Rana Faris Salman¹, Basma Talib Al-Sudani^{2*}, Bahir Abdul Razzaq Mshimesh¹

¹Department of Pharmacology and Toxicology, College of Pharmacy, Mustansiriyah University, Iraq.

²Department of Clinical Laboratories Sciences, College of Pharmacy, Mustansiriyah University, Iraq.

***Corresponding author:** Basma Talib Al-Sudani, Department of Clinical Laboratories Sciences, College of Pharmacy, Mustansiriyah University, Iraq,
Email: basma_alsudani@uomustansiriya.edu.iq

Submitted: 14 January 2023; Accepted: 18 February 2023; Published: 07 March 2023

ABSTRACT

The skin is the largest organ of the body. The general aging process, which is genetically fixed and happens solely with the passage of time, is referred to as the intrinsic skin aging process. The skin aging process caused by external causes is referred to as extrinsic skin aging. The skin must endure a continual bombardment from the outside by reactive oxygen species, or ROS, which are given to the skin by the environment and created within the skin itself, either as a reaction to incoming UV radiation or made when mitochondria aerobic respiration. An increase in the levels of ROS lead to damage the mtDNA, affecting cell signaling and inducing the apoptosis responses, such as senescence, fibrosis, calcification, and hypertrophy. During the past decade, investigators have reported the relationship between disturbance of SIRT1 activation and the onset of aging. Sirtuin1 is indispensable for DNA repair which make it good anti-senescence/anti-ageing targets and because ROS and SIRT1 are disturbed in the aging process. Because of its enhancing effect on reactive oxygen species and apoptotic pathways, an aberrant increase in NO generation has been linked to early skin aging. We'll look at how SIRT1 aptamer (as a SIRT1 activator) can protect cells against sodium nitroprusside-induced cell death (SNP), employing a human keratinocyte cell line to study a well-known NO generating chemical with suspected harmful and apoptotic effects on keratinocytes (HaCaT). As a result, the primary goal of this research is to discover and define the protective effects of SIRT1 activators in human skin cells. Finally, the findings imply that SIRT1 aptamer might be effective in preventing skin aging caused by reactive oxygen species (ROS).

Keywords: *Reactive oxygen species, Human keratinocytes cell line (HaCaT), SIRT1 aptamer, Apoptosis*

INTRODUCTION

SIRT1 regulates multiple pathways through enhancement of defense system of the skin against oxidative stress and other factor involved

in skin aging. The ROS and RNS that are produced in the skin as a result of UV exposure, air pollution, and other factors that induce sunburn and damage cellular DNA are known as reactive oxygen species (ROS and RNS).

Cellular senescence, apoptosis, and carcinogenesis are all on the rise (1) (Figure 1). ROS promote collagen breakdown by activating tissue remodeling matrix metalloproteinases (MMPs) in the skin layers, which is the result of DNA damage which is not repaired properly (2). Upregulation of SIRT1 decreases UVB-induced oxidative stress and apoptosis, according to previous study (3). UVB radiation reduces epidermal SIRT1 expression, which causes the acetylated p53 protein to induce apoptotic cell death (4). Therefore, SIRT1 overexpression provides protection to fibroblasts from UVB-

induced cell senescence by influencing the transcriptional activity of p53 via the deacetylation process and oxidative status (3). Accordingly, we hypothesize that SIRT1 aptamer (as SIRT1 activator) could exert its protective actions through reducing the abnormal increase in the level of NO following exposure to ultraviolet radiation. SIRT1 aptamer is a novel SIRT1 ligands (DNA sequences consist of 40 nucleotides) that bind and modulate the activity of SIRT1 within cells and enhance its enzymatic activity which is used NAD⁺ to remove acetyl groups from proteins (5).

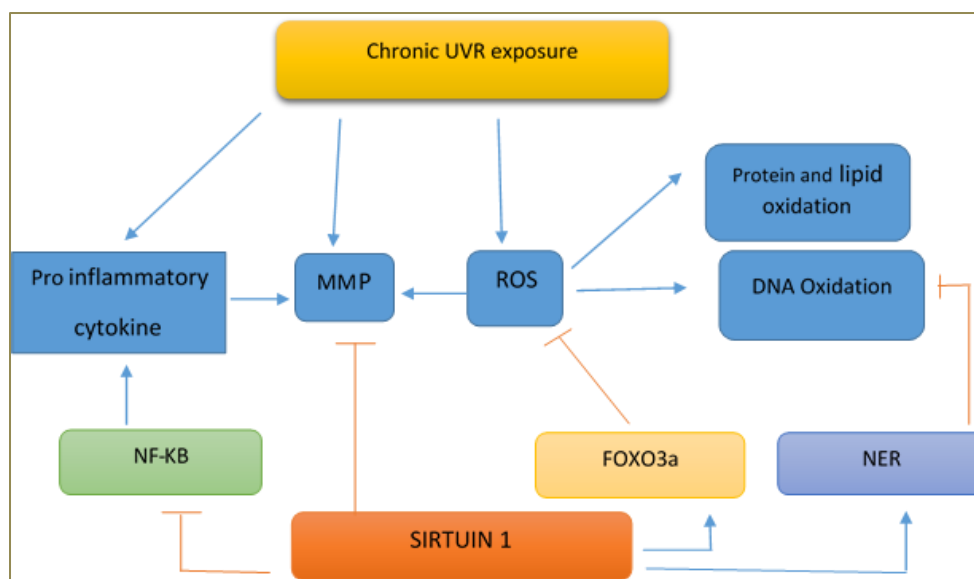


FIGURE 1: UV radiation affects skin aging in a variety of ways. (MMPs means for matrix metalloproteinases, and ROS represents for reactive oxygen species.) UVR stands for ultraviolet radiation, MMPs for matrix metalloproteinases, and ROS for FOXO3 refers for Forkhead Box O3 alpha; NER stands for nucleotide excision repair system; SIRT1 represents for Sirtuin 1 (6).

SIRT1 aptamer is the new revolutionary method of a novel therapy that may be helpful in treating various aging-related diseases because it has anti-inflammatory, anti-type 2 diabetes, and anti-cancer effect (7-13). SIRT1 structure is modified by aptamer-SIRT1 interaction, which enhances binding activity with substrates such as p65/RelA (KD value = 27.07 0.959 nM) and activates multiple targets (12). The role of SIRT1 aptamer as an immune response modulator was demonstrated in both in vitro and in vivo studies (7-11), It increased immunological activity against cancer cells and reversed immune

senescence in rats (12). All these effects are due to its ability to remove ROS (13). In addition to that, SIRT1 aptamer was tested for both cancer and normal cells and SIRT1 aptamer show selected activity against cancer cells that had elevated level of SIRT1 and this selectivity is absent in Resveratrol and the SIRT1 activators compounds. This means; SIRT1 aptamer has the advantage over chemotherapy in selectivity against cancer cells with high limitation of adverse effects associated with chemotherapy (5,13). In toxicology studies, neither activation of the immune system, nor complement activation

by SIRT1 aptamer was reported. The identification of SIRT1 aptamer as a potential anti-aging medicine with a slew of other health benefits has stimulated research into its protective effects against variables that influence the course of natural skin aging. Researchers will explore the protective benefits of SIRT1 aptamer (as SIRT1 activator) against cell death produced by sodium nitroprusside (SNP), a well-known NO producing compound with putative toxic and apoptotic effects on keratinocytes, using a human keratinocyte cell line (HaCaT). As a result, the primary goal of this research is to discover and define the protective effects of SIRT1 activators in human skin cells. Finally, the findings imply that SIRT1 aptamer might be effective in preventing skin aging caused by reactive oxygen species (ROS).

MATERIALS AND METHODS

Materials

CLS Cell Lines Service provided human HaCaT keratinocytes for this study (Germany). Lonza provided the materials for the cell cultures (UK). Fluorescent dyes: calcein from Thermo Scientific (USA), SYTO16 green from Invitrogen (Germany), Sigma-Aldrich Ltd provided JC-1 from Abcam (UK) and Griess reagent kit (USA). Abcam (UK) provided the Caspases -9 colorimetric test kits, while Bioscience provided the reactive oxygen species (ROS) assay kit (USA). All other chemicals were bought from Sigma-Aldrich (USA) unless otherwise noted. The aptamer that activator SIRT1 (BAS aptamer) was collected from BioNeer Company-Korea at 200 μ M. BAS aptamer-based system in structured 40-base that sequence (5'CGGACTGCAACCTATGCTATCGTTGATGTCTGTCCAAGCA-3') (5) for high binding affinity against SIRT1 enzyme with KD value = 48.3 nM and IC50= 5 μ M. According to IC50, the concentrations of SIRT1 aptamer that used in all experiments were 1.25, 2.5, 5, 10 μ M. These concentrations were prepared in water nuclease-free inside the sterile hood to avoid any contamination. In dimethylsulfoxide, stock solutions of SIRT1 aptamer and other medicines were dissolved (DMSO). At 0.03 percent (v/v),

this solvent has no influence on cell viability.

Cell culture

HaCaT cells were cultured in DMEM with high glucose, 10% fetal bovine serum (FBS), and 1% penicillin/streptomycin in HEPES-buffering Dulbecco's modified Eagle medium (DMEM). The cells were grown by taking out the DMEM medium twice a week and replaced it with the same amount DMEM medium until they reached 90% confluence. Cells were then removed from 75 cm³ culture flasks using 0.25 percent trypsin in 0.02 percent EDTA-PBS and transplanted into 6 well and 96 well plates (Falcon, USA). After reaching confluence, the cultures were stored at 37°C in a humidified atmosphere (5 percent CO₂ and 95 percent air) and used for research.

SIRT1 aptamer protects HaCaT cells against SNP-induced toxicity

Nitric oxide free radical donor (Sodium nitroprusside SNP)- In HaCaT cells plated in 96 wells, induced toxicity was tested. Accordingly, human HaCaT cell lines were divided into four main groups (96 well plate at 24h):

- 1- Control group: HaCaT cell lines were cultured in normal conditions.
- 2- 0.3mM SNP group: HaCaT cells were pretreated with 0.3mM sodium nitroprusside (SNP) before adding SIRT1 aptamer at 0, 1.25, 2.5, 5, 10 μ M.
- 3- 1mM SNP group: HaCaT cells were pretreated with 1mM sodium nitroprusside (SNP) before adding SIRT1 aptamer at 0, 1.25, 2.5, 5, 10 μ M.
- 4- 3mM SNP group: HaCaT cells were pretreated with 3mM sodium nitroprusside (SNP) before adding SIRT1 aptamer at 0, 1.25, 2.5, 5, 10 μ M.

The DMEM medium was withdrawn on the day of the experiment and replaced with a comparable mixture containing 0.3, 1, 3.0 mM SNP and no FBS in the presence or absence of various medications. The calcein AM and 3-(4,5-dimethylthiazol-2-yl)-2,5-diphenyl tetrazolium bromide (MTT) tests were used to measure cell survival 24 hours later.

MTT assays

After cultured HaCaT cell lines, viewed the cells using an inverted microscope to assess the degree of 80 % confluences and confirmed the absence of bacterial and fungal contaminants, then removed and discard culture medium. Rinsed the cell layer with 5 ml of Dulbecco's PBS without Ca²⁺/Mg²⁺ solution to remove all traces of serum that contains trypsin inhibitor and repeated this step 3 times. Added 3 ml of trypsin-EDTA solution to the flask to cover the cells and extract gently with a pipette the excess of the trypsin-EDTA solution and leave enough solution to cover the cell monolayer and incubate 3 minutes at 37°C and checked periodically for cell detachment, then observed cells under an inverted microscope until cell layer is dispersed. 5 ml of complete growth medium was added to aspirate cells by pipetting and centrifuged in a sterile 15 ml sterile centrifuge tube at 200 rpm for 5 min. After that counted the cells viability by trypan blue staining. After trypsinization, diluted a lot HaCaT cells to 50000 cells/ml by used complete media, then prepared a 96 clear sterile cell culture plate and added 100 µl of the 50,000 cells/ml solution into each well, this gave 5000 cells/well and incubated overnight in the incubator (37°C – 5% CO₂). On the dosing day, prepared a second well plate to transfer 5µl from SNP groups to 125µl of warmed up media of each well plate by a multichannel. To each well of cells, added 25 µl of SNP groups with media from second plate for HaCaT cells plates. After 12h, SIRT1 aptamer at 0, 1.25, 2.5, 5, 10µM was added and incubated overnight. In the next day, removed the plate from the incubator and placed it in the safety cabinet. Added 30 µl of MTT solution to each well, then mixed the plate in the thermo mixer for 2 minutes at 500 rpm at 37°C. Incubated for 4h at 37°C in culture hood. Finally, read absorbance at 500-600 nm (14).

Calcein assay

After cultured HaCaT cell lines, and reached to 80 % confluences, removed culture medium and rinsed the cell 5 ml of PBS 3 times. Added 3 ml of trypsin-EDTA solution to the flask and incubated 3 minutes at 37°C, then observed cells

under an inverted microscope until cell layer is dispersed. 5 ml of DMEM medium was added to aspirate cells and centrifuged at 200 rpm for 5 min. After that counted the cells viability by Trypan blue staining and seeded HaCaT cells to 100000 cells/ml by used complete media, then prepared a 96 black plate and added 100 µl of the 100,000 cells/ml solution into each well, this gave 10000 cells/well and incubated overnight in the incubator (37°C – 5% CO₂). On the dosing day, prepared a second well plate to transfer 5µl from SNP groups to 125µl of warmed up media with 1 x Hank's balanced salt solution and 20 mM HEPES (HHBS) of each well plate by a multichannel. To each well of cells, added 25 µl of SNP groups with media from second plate to HaCaT cells plates. After 12h, SIRT1 aptamer at 0, 1.25, 2.5, 5, 10µM was added and incubated overnight. In the next day, added 100 µl of Calcein AM dye solution to each well and mixed to avoid cross-contamination, then incubated for 30 minutes at 37°C in culture hood. At the end, read fluorescence on fluorescence plate reader at excitation wavelength set at 485 nm and emission wavelength at 530 nm (15).

In Vitro evaluation the apoptotic HaCaT nuclei by SYTO 16 staining assa

Nuclear staining was performed using the fluorescent nuclear dye SYTO 16. This method has been validated as an indicator of apoptotic cell death (16). Briefly, seeded HaCaT cell lines at 25000 cells/well in 12 well plate. Following a 24h HaCaT cells were exposure to 25µl from SNP (0.3–3 mM), after 12h, 50µl from SIRT1 aptamer at 0, 1.25, 2.5, 5, 10µM were added to each well and incubated overnight. On the testing day, the growth media was withdrawn, and HaCaT cells were incubated for 30 minutes at 37°C in phenol-free DMEM medium containing SYTO 16 (2 M). The increased SYTO 16 staining was utilized to automatically measure the amount of apoptotic HaCaT cells using a microplate fluorescence reader (excitation = 485 nm; emission wavelength @ 530 nm). Finally, a microscopic investigation utilizing an Optika microscope for cell imaging was performed.

Measurement the detection changes in mitochondria membrane potential ($\Delta\Psi$) by flowcytometry

1×10⁴ HaCaT cells were plated in 24 well plate contained 100µl DMEM media and allowed to attach overnight. SNP at different concentration (0.3, 1, 3 mM) were prepared in buffer solution and diluted in complete media with 10% FBS without phenol red and treated the HaCaT cells with it. Following a 24h, culture medium was removed and detached the cells with 0.5 mM EDTA, which is gentler than trypsinization. The HaCaT cells were washed once with serum-containing media prior to incubated with 100µl/well JC-10 dye-loading solution (3 µM) for 10 minutes at 37°C in the dark included blank wells (with non-stained cells). After that, HaCaT cells were washed twice with 100µl/well of 1X dilution buffer and treated with 25 µl SIRT1 aptamer at 0, 1.25, 2.5, 5, 10µM include 10µM CCCP as a positive control and incubate for 4h at 37°C. Finally, monitored the fluorescence intensity by used a flow cytometry and florescent microscopy in FL1 channel for the green fluorescent monomeric signal (in apoptotic cells), and the FL2 channel for the red fluorescent aggregated signal (in healthy cells). The intensity ratio of FL1 to FL2 was used to monitor the mitochondria membrane potential change induced by the aptamer treatment. CCCP was used for compensation corrections. Additionally, read plate end point in the presence of SIRT1 aptamer, media on a fluorescent plate reader with set excitation wavelength at 535 ± 17.5 nm and emission wavelength at 590 ± 17.5 nm (17).

Measurement of intracellular ROS accumulation

Intracellular reactive oxygen species (ROS) production was measured by ROS assay kit is a cell-based assay for measuring hydroxyl, peroxy, and other reactive oxygen species activity within a cell. 1ml HaCaT cells suspensions were dispensed into 12-well flat clear-bottom dark sided tissue culture plates at concentrations of 25,000 cells per well and incubated 24h under standard conditions. At the start of 1 and 3 mM SNP treatment, the freely permeable DCFH-DA was added to the culture medium. After 24 hours, the HaCaT cells were

washed in 100l/well 1x buffer and subjected to 50 M TBHP (Tert-Butyl Hydrogen Peroxide) for 6 hours before being treated with 1.25, 2.5, 5, or 10 M SIRT1 aptamer. The cell culture media was withdrawn after a 5-hour recovery time, and the rinsed thoroughly in 100 l/well 1x buffer, then 1x buffer was withdrawn, and the cells were dyed by adding 100 l/well of the DCFDA solution (10 l of 20 Mm DCFDA solution with 10 ml 1X buffer). At 37° C, the culture was incubated for 45 minutes with the DCFDA solution. After that, the DCFDA solution was withdrawn and 100 l/1X buffer was added to each well. With an excitation wavelength of 485 nm and an emission wavelength of 535 nm, fluorescent units were evaluated in each well using a luminometer microplate reader's fluorescence measuring system (18).

Measurement of nitrite formation

HaCat cells were seeded in 24-well plates (2 × 10⁶ cells in 2 ml per well) and rested for 24 h to allow attachment to the well surface, then HaCaT cells were exposed to 1 and 3 mM SNP at 4h. After that, DMEM media was changed and treated the cells with 1.25, 2.5, 5, 10 µM SIRT1 aptamer in DMEM without FBS. Concentrations of nitrite, the end-product of NO production, was quantified 5 hours later by added 10 µl of Griess reagent (N-(1-naphthyl) ethylenediamine and sulfanilic acid) to HaCaT cell culture medium that treated and incubated at room temperature for 10 minutes with protected from light. A purple/magenta color was beginning to form immediately. After 30 minutes, the optical density at 544 nm was determined using a microplate reader. The optical density of a nitrite solution made in culture media was used to calculate nitrite concentrations. In culture media, the detection limit for nitrite measurement was 1 M (19).

Estimation the Caspases-9 activity

Caspase-9, a cysteine-aspartic protease known for its role as an initiator of intrinsic apoptosis, regulates physiological cell death and pathological tissue degeneration. Caspase-9 activity was detected using the caspase-9 colorimetric assay kit. The assay is based on

spectrophotometric detection of the chromophore p-nitroanilide (p-NA) after cleavage from the labeled substrate LEHD-p-NA. The p-NA light emission was quantified using a microliter plate reader at 400 or 405 nm (20). Following the manufacturer's protocol, briefly, 5×10^6 HaCaT cells were incubated in 6 well plate with SNP at a concentration 0.3, 1, and 3 mM alone during 24h and with 1.25, 2.5, 5, 10 μ M SIRT1 aptamer. Re-suspended cells in 50 μ l of chilled Cell Lysis Buffer and incubated cells on ice for 10 minutes. After that, centrifuged for 1 min in a micro centrifuge (10,000 x g) and transferred the supernatant (cytosolic extract) to a fresh tube and put on ice to measure the protein concentration by BCA protein colorimetric assay kit. Firstly, serial concentration was prepared to get standard curve dilute by added 0, 0.2, 0.3, 0.4, 0.6, 0.7, 0.9, 1 mg/mL from BCA standard solution with normal saline. In 96 well plate, 20 μ l of standard solution at different concentration was added. Secondly, 18 μ L PBS and 2 μ L samples supernatant were added to 200 μ l of BCA working solution to the wells. Mixed for 20 second and incubated at 37°C for 30 min. Finally, measure the OD value of each well at 562 nm with micro plate reader. Then calculated the protein concentration in each samples. Total protein amount of samples between 70-100 μ g. Fifty micrograms of the total protein (cytosolic extract) were utilized for the estimation of caspase -9. 50 μ l reaction buffer (containing 10 mM DTT) was added to all cytosolic extract samples in the presence of 5 μ l capase-9 substrate (4 mM LEHD-p-NA) and incubated at 37°C for 2 h. A micro-plate reader was used to quantify the optical density at 405 nm after 2 hours. The optical density of a p-NA standard produced in

buffer was used to evaluate caspase-9 concentrations.

Statistical analysis

All statistical analysis of data was performed using software Prism 8 software. A comparison between all groups within the same plate of MTT, Calcein assay, ROS levels, nitrite formation, JC-1 assay to were evaluated by one-way ANOVA with Tukey (Prism 8 software). Statistically significant values considered $p < 0.05$.

RESULTS

SIRT1 aptamer protects HaCaT cells against SNP-induced toxicity

This experiment was performed a functional assay to evaluate the capacity of SIRT1 aptamer to protect HaCaT cells against the toxicity induced by the NO releasing SNP (SNP IC₅₀= 1.5mM). The IC₅₀ of SIRT1 aptamer was 5 μ M as mentioned in section 2.2.1.4. Treatment of HaCaT cells with SNP (0.3–3 mM) inhibited the growth of HaCaT cells in a concentration dependent manner, as evaluated by the MTT and Calcein assays (Figure 1 and 2). Both assays showed that SIRT1 aptamer at different concentrations (10, 5, 2.5 μ M) strongly attenuated 3mM SNP-induced toxicity by 100, 97 and 80% respectively $p < 0.05$ as compared with untreated SIRT1 aptamer group (29% cell survival) in MTT assay and by 99, 79 and 59% respectively in Calcein assay as it was more accurate and sensitive test for determined the toxicity of biotherapy drug, producing a significant effect at 10 μ M and a maximal one at the highest concentration tested.

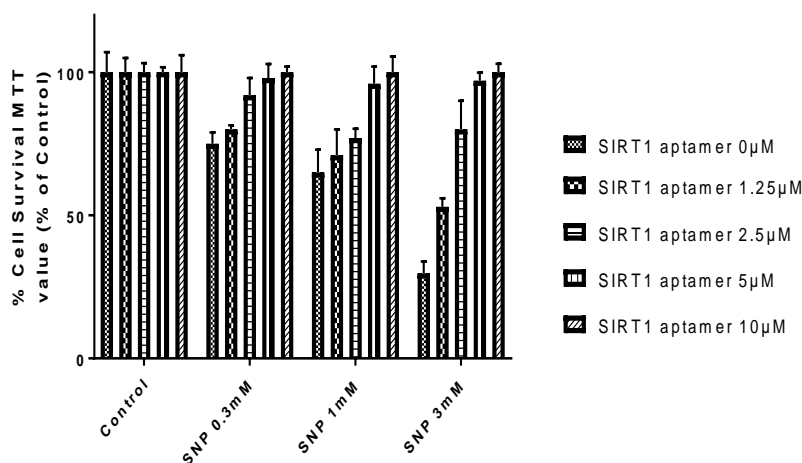


FIGURE 1: SIRT1 aptamer's effect on HaCaT cell death caused by SNP. SNP (0.3–3 mM) was given to HaCaT cell lines in the presence or absence of SIRT1 aptamer (10, 5, 2.5, 1.25, 0M). MTT tests were used to measure cell vitality 24 hours later. The mean SEM of at least three different experiments is shown by the values.

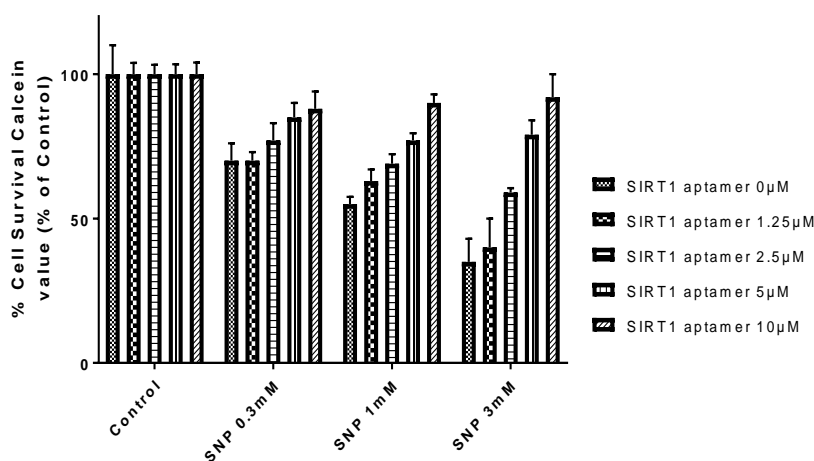


FIGURE 2: Effect of SIRT1 aptamer against HaCaT cell death induced by SNP. HaCaT cell lines were exposed to SNP (0.3–3 mM) in the presence or absence of SIRT1 aptamer (10, 5, 2.5, 1.25, 0 μM). Cell viability was determined 24 hours later using Calcein assays. Values represent mean ± SEM of at least three separate experiments.

In Vitro evaluation the apoptotic HaCaT nuclei by SYTO 16 staining assay

The number of apoptotic HaCaT cells that treated with SNP and stained with SYTO 16 were increased, indicating that SNP exerted an apoptotic effect on HaCaT cells (Figure 3). The

increase in apoptotic HaCaT cell lines was reduced when treated with SIRT1 aptamer (10, 5, 2.5, 1.25 μM) with a significant inhibitory effect of apoptotic at 5 μM and more from 266% to 140% p< 0.05 (Figure 3 and 4).

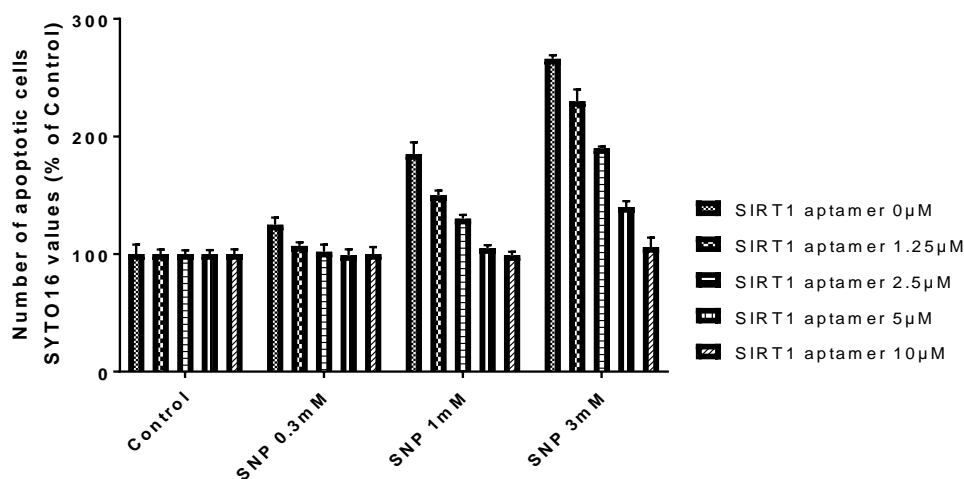


FIGURE 3: Effect of SIRT1 aptamer against apoptotic events induced by SNP in HaCaT cells. HaCaT cells were exposed to SNP (0.3–3 mM) in the presence or absence of SIRT1 aptamer (10, 5, 2.5, 1.25, 0 μM). HaCaT cells viability was determined 24 hours later using the SYTO 16 assay. Values represent mean ± SEM of at least three separate experiments.

As SYTO 16 is a sensitive DNA stain and broadly used for viability studies. Accordingly, the SYTO 16 dye easily penetrates HaCaT cells and undergoes dramatic fluorescence enhancement upon binding to nucleic acids.

Thus, when HaCaT cells were incubated with SYTO 16, the nuclei from living cells were stained in green (Figure 4). Cells that did not display any nuclear green fluorescence were considered as non-viable.

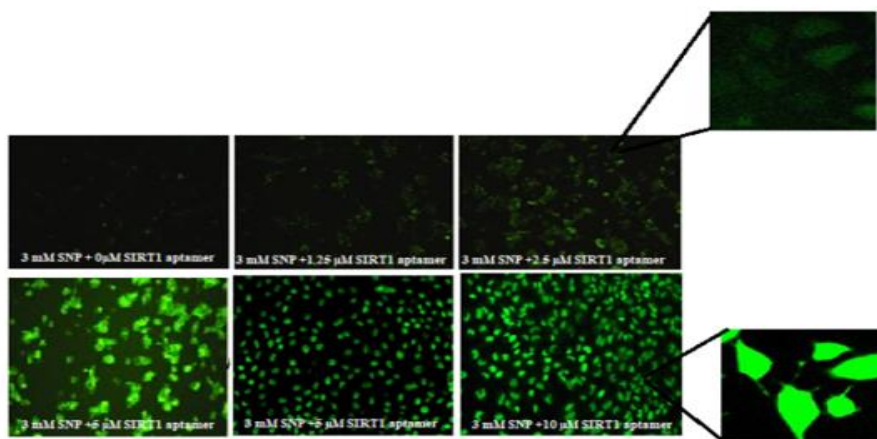


FIGURE 4: Effect of SIRT1 aptamer against apoptotic events induced by SNP in HaCaT cells. HaCaT cells were exposed to 3 mM SNP with 0, 1.25, 2.5, 5 and 10 μM SIRT1 aptamer at 24h using the SYTO 16 assay.

Measurement the detection changes in mitochondria membrane potential ($\Delta\Psi$) by flowcytometry

The JC1 assay confirmed the apoptotic effect of SNP resulting in the loss of mitochondrial

membrane potential (MMP) by floctometry as shown in figure 5. The results demonstrates 98% of untreated HaCaT cells with aptamer or SNP (control) were available. While, the % $\Delta\Psi$ M of HaCaT cells that exposed to 0.3,1,3 mM SNP

was significantly increased to reached about 70% (red color down); when HaCaT cells pretreated with (10, 5, 2.5, 1.25 μ M) SIRT1 aptamer followed by treatment of 3mM SNP, the 5 and 10 μ M SIRT1 aptamer were attenuated NO-

induced mitochondrial membrane potential loss in HaCaT cells. Figure 6 shows the % of apoptotic density of HaCaT cells relative to mitochondrial membrane potential.

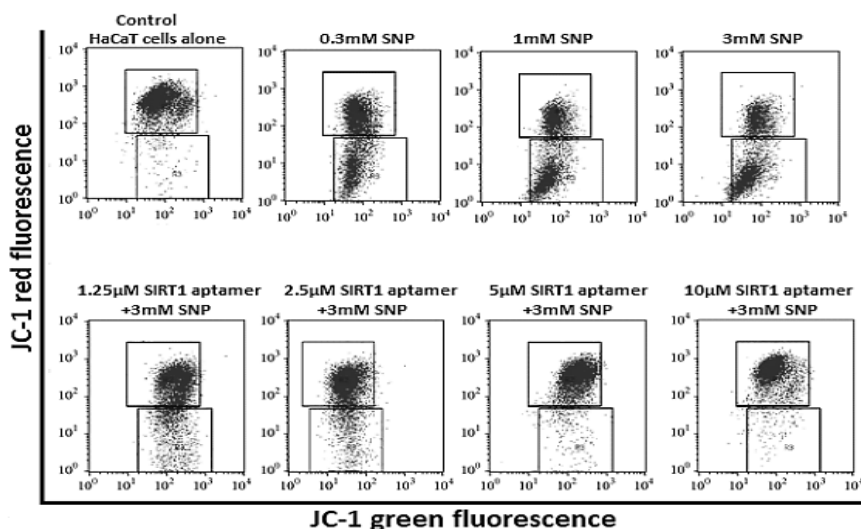


FIGURE 5: SIRT1 aptamer attenuated NO-induced mitochondrial membrane potential loss in HaCaT cells, as assessed by JC-1 staining. (a) HaCaT cells without aptamer or SNP (control); (b-d) HaCaT cells exposed to 0.3,1,3 mM SNP; (e)–(h) HaCaT cells pretreated with (10, 5, 2.5, 1.25 μ M) SIRT1 aptamer followed by treatment of 3mM SNP. Values are expressed as mean \pm SD from three independent experiments.

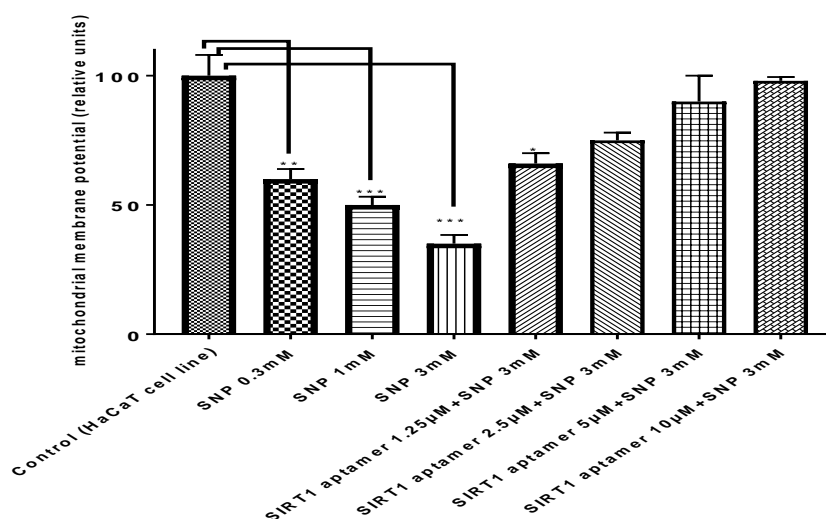


FIGURE 6: Effect of SIRT1 aptamer against apoptotic events induced by SNP in HaCaT cells. Cells were exposed to SNP (0.3–3 mM) in the presence or absence of SIRT1 aptamer (10, 5, 2.5, 1.25 μ M). Cell viability was determined 24 hours later using both the JC-1 assays. Values represent mean \pm SEM of at least three separate experiments. ** p <, 0.005, *** p <0.01 compared between groups treated with SNP alone and control. * p <0.05 compared groups treated with SNP+ 1.25 μ M SIRT1 aptamer with control group

Figure 7 shows the HaCaT cells imaging by florescent microscopy as indicated the decreased mitochondrial membrane potential in the red/green fluorescence intensity ratio. 5µM SIRT1

aptamer reversed the loss of MMP, with significant effect at the concentrations with an anti-apoptotic effect.

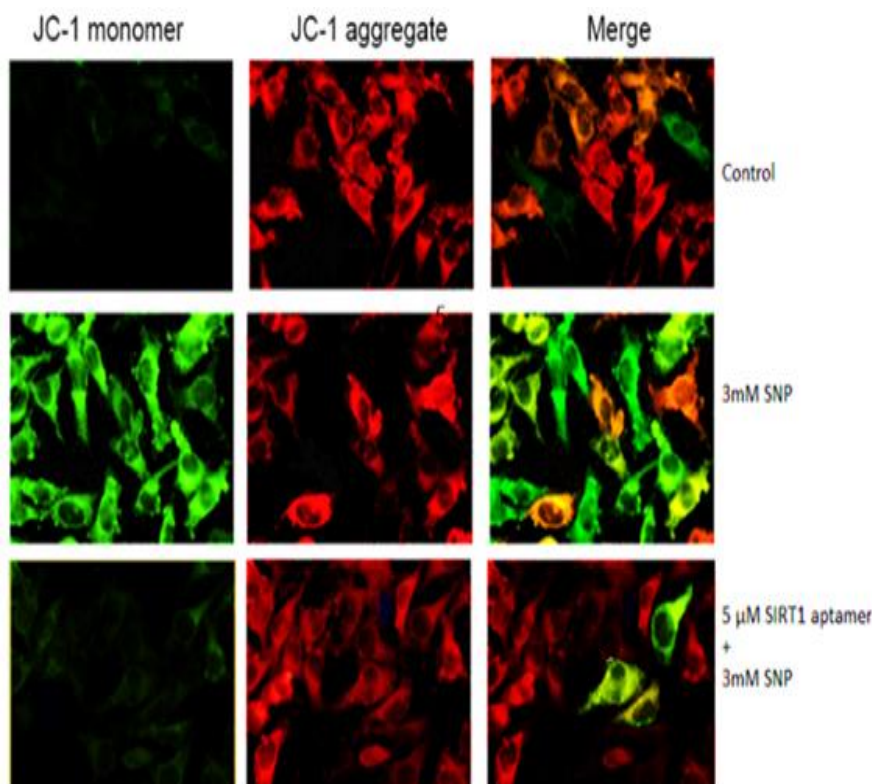


FIGURE 7: Mitochondrial membrane potential measurement by JC1 on HaCaT cells (1) Control (HaCaT) cells; (2) HaCaT cells treated with 3mM SNP (3) HaCaT cells pretreated with 5µM SIRT1 aptamer followed by treatment of 3mM SNP which clearly indicates the SIRT1 aptamer can reduced the loss of NO-induced mitochondrial membrane potential in a dose-dependent manner.

To sum up, the mitochondrial membrane potential was markedly decreased in HaCaT cells treated with 0.3-3mM SNP for 1 h, indicating that NO treatment induced mitochondrial dysfunction. SIRT1 aptamer pretreatment significantly reduced the loss of NO-induced mitochondrial membrane potential in a dose-dependent manner.

Measurement of intracellular ROS accumulation

The fluorescent dye 2,7-dichlorofluorescein diacetate (5 mM DCF) was used to measure

intracellular ROS levels in conjunction with cell survival. The DCF experiment revealed that a 5-hour exposure to SNP (1 and 3 mM) resulted in an increase in ROS formation (Figure 8). SIRT1 aptamer (10, 5, 2.5, 1.25M) significantly reduced SNP-stimulated ROS production by 125,250, 290, and 315 percent, respectively, whereas ROS accumulation in cell cultures treated with SIRT1 aptamer (10, 5, 2.5, 1.25M) alone was slightly, but significantly reduced in untreated SNP groups, indicating that SIRT1 aptamer protected cells against SNP-induced toxicity (Figure 8).

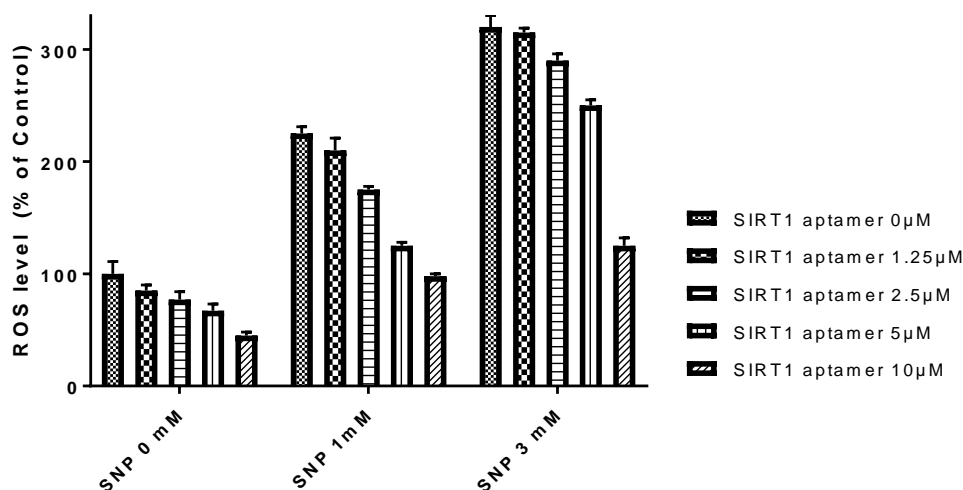


FIGURE 8: Effect of SIRT1 aptamer against ROS level induced by SNP in HaCaT cells. Cells were exposed to SNP (1 and 3 mM) in the presence or absence of SIRT1 aptamer (10, 5, 2.5, 1.25 μM). ROS level was determined 5 hours later using the DCF assay. Values represent mean ± SEM of at least 3 separate experiments.

Figure 9 shows the decreased level of fluorescent ROS accumulation in fluorescence microscopy of HaCaT cells which were significantly affected by SIRT1 aptamer at 5 μM (vs SNP 3 mM) and 10 μM (vs SNP 3 mM).

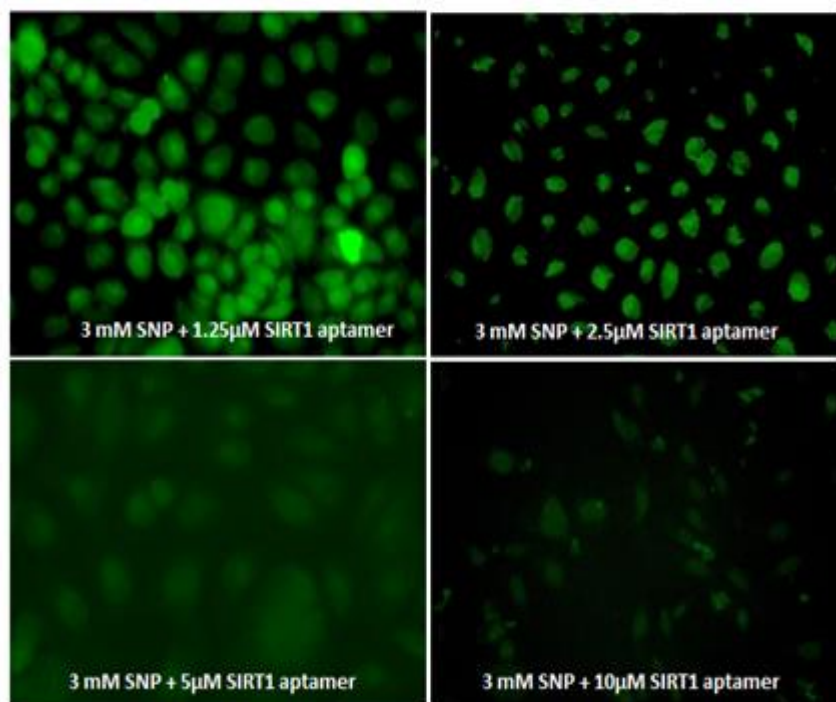


FIGURE 9: Effect of SIRT1 aptamer against ROS level induced by SNP in HaCaT cells. Cells were exposed to 3 mM SNP SIRT1 aptamer at (10, 5, 2.5, 1.25 μM). ROS level was determined by fluorescence microscopy using the DCF assay.

Measurement of nitrite formation

To evaluate the ability of SIRT1 aptamer to modulate the activity of nitric oxide synthase (NOS) elicited by SNP, the nitrite accumulation was measured. The results as shown in figure 3-10 indicated that SIRT1 aptamer could be worked as a protective action by directly

associated to the inhibition of NOS that induced by 4-hour exposure the HaCaT cells to SNP (1–3 mM) by decreased nitrite level in the culture medium ($P < 0.001$). Moreover, SIRT1 aptamer at 5 and 10 μM was successfully to attenuate NO production at the concentrations that protected HaCaT cells against SNP (Figure 10).

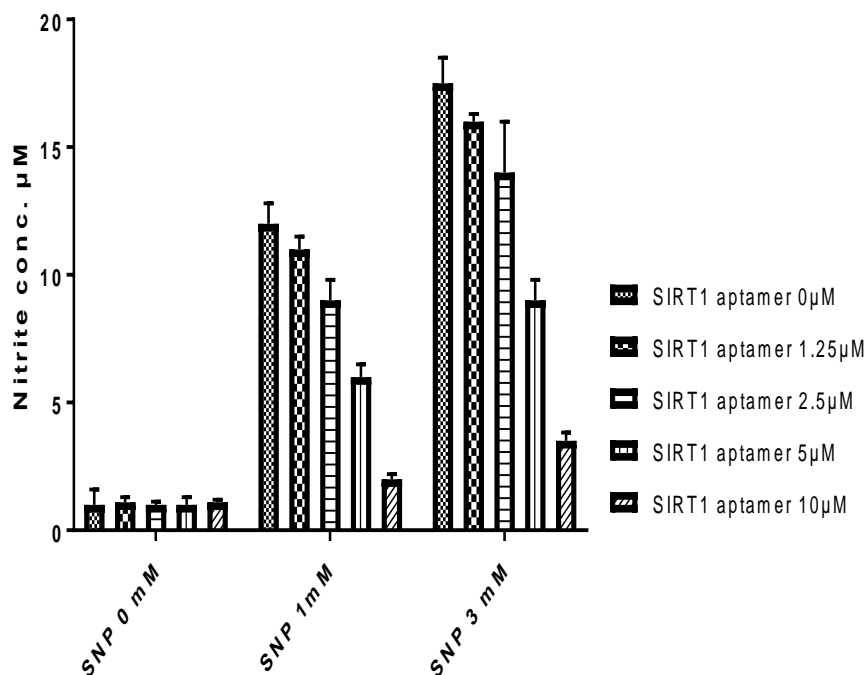


FIGURE 10: Effect of SIRT1 aptamer on NO levels in HaCaT cells caused by SNP. In the presence or absence of SIRT1 aptamer (10, 5, 2.5, 1.25M), cells were exposed to SNP (1 and 3 mM). The Griess reagent test was used to assess NO levels four hours later. The values represent the mean SEM of at least three different experiments.

Estimation the Caspases-9 activity

ELISA corroborated a function for caspases-9 in NO-induced apoptosis in HaCaT cells, since SNP (0.3–3 mM) elevated caspases-9 activity, with a significant impact at 3 mM (Figure 11). SIRT1

aptamer decreased caspase-9 activity in a concentration-dependent manner, with a substantial impact at 10 M. (Figure 11). Furthermore, the SIRT1 aptamer totally blocked SNP-induced caspase-9 activation.

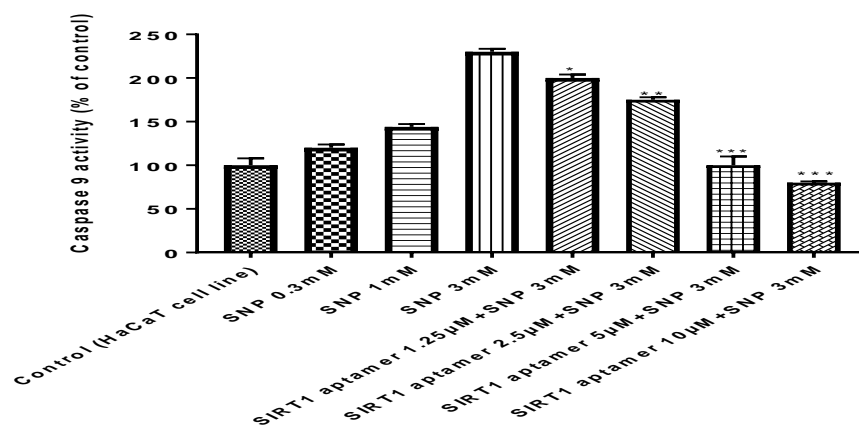


FIGURE 11: SIRT1 protects HaCaT cells against SNP-induced caspase-9 activation. SNP (0.3– 3 mM) was given to cells in the presence or absence of SIRT1 aptamer (10, 5, 2.5, 1.25M). Colorimetric test kits were used to evaluate caspase-9 activity 24 hours later. The values represent the mean and standard deviation of at least three different experiments. **p<0.001 as compared to those given 3mM SNP alone.

DISCUSSION

The significant protective benefits of SIRT1 aptamer against toxicity generated by NO releasing SNP are described for the first time in this work. SIRT1 aptamer protected HaCaT cells exposed to SNP, demonstrating its capacity to inhibit the detrimental events triggered by NO overproduction, a mechanism linked to premature skin aging caused by long-term UV exposure, according to the findings. (21). In current study, when compared to its reaction with the superoxide anion radical, which produces extremely harmful reactive oxygen species, its reaction produces antioxidant characteristics (peroxynitrite). This molecule is broken down to create nitrogen dioxide and the hydroxyl radical, both of which cause DNA damage. (22). MTT and Calcein used to evaluate the protection capacity of SIRT1 aptamer against the toxicity generated by NO release from SNP in HaCat cell line. The MTT assay was performed to determine whether of SIRT1 aptamer was toxic to HaCat cells. In the current study the percentage of cell death and toxicity decrease with SNP in dose dependent manner, SIRT1 aptamer strongly attenuated SNP-induced toxicity with significant effect at (2.5 µM, 5 µM and 10 µM) strongly attenuated 3mM SNP-induced toxicity by 100, 97 and 80% respectively $p < 0.05$ as compared with untreated SIRT1 aptamer group (29% cell survival). This indicate that SIRT1 aptamer has a

significant protective effect against oxidative stress-induced cytotoxicity by SNP in HaCat cells suggesting its ability to block the deleterious events induced by NO overproduction by inhibiting apoptosis pathway. The current study agrees with pervious study which used SIRT1 activator (Resveratrol) show potent protective effects in various models of toxicity including toxicity induced by NO releasing SNP (23). In this study Calcein-AM is a lipophilic compound that diffuses through the intact cell membrane and stains the cytoplasm (green fluorescence) after the calcein moiety is freed by endogenous esterase which is accurately proportional to cells viability when endogenous esterase hydrolyzes calcein moiety to a hydrophilic, strongly fluorescent compound that is well-retained in the cell cytoplasm (24) Calcein -AM is more accurate than MTT for studying of cell viability and cellular cytotoxicity due to its superior cell retention and relative insensitivity of its fluorescence to pH in the physiologic range (25). Maximum calcein fluorescence intensity at producing a significant effect at concentrations (10, 5, 2.5µM) and toxicity strongly attenuated by 99, 79 and 59% respectively figure (2) and a maximal one at the highest concentration tested. Our result in current study shown the superiority of SIRT1 aptamer in protection of HaCat against cytotoxic effect of SNP regarding other SIRT1 activator cell viability percentage was 70%

competing with 90% of cell viability when SIRT1 aptamer has been applied (23). To investigate the effects of SIRT1 aptamer on HaCat cell line in presence of strong NO donor SNP, SYTO dyes were used. It is a cell-permanent nucleic acid stain that shows a large fluorescence enhancement upon binding nucleic acids (26). SYTO dyes differ from each other in one or more characteristics, including cell permeability, fluorescence enhancement upon binding nucleic acids, SYTO 16 stain used for detecting apoptosis when it's screened for the ability to discriminate between apoptotic and non-apoptotic cells do not interfere with cell viability (27). Apoptosis is a kind of programmed cell death that has been associated with cell loss, RNS like NO is a potent apoptotic agent that can cause cell death. Apoptotic cell death affects keratinocyte growth and the development of the stratum corneum in the skin (28). Caspases are cysteine-dependent aspartate-specific proteases that are involved in the production, transmission, and amplifying of apoptotic signals in cells (29). Several mechanisms are involved in the apoptotic pathways in keratinocytes, all must, however, pass via the caspase family. Caspases are activated in a specific order during apoptosis (30). The results revealed that SNP at a high concentration (3mM) promotes cell apoptosis, consistent with earlier studies (23,31,32). Figure 4 shows gradual decrease in SYTO 16 fluorescent in dose dependent manner, when SIRT1 aptamer at dose (10 μ M) green fluorescent almost disappeared and shown maximum fluorescent at dose (1.25 μ M) that may be explained as increased SYTO16 fluorescence during apoptosis is caspase-dependent and the decrease of SYTO16 fluorescence was attributed by pharmacological inhibition of Caspases (33). SIRT1 aptamer significantly inhibits the effect of apoptotic at dose (5 μ M) with % ($p < 0.05$) (Figure 3). SIRT1 has a role in the anti-apoptosis pathway, which has been proven in a number of previous studies (34). The current findings showed that enhanced SIRT1 expression by SIRT1 aptamer resulted in a decrease in the number of apoptotic cells when compared to the control, suggesting that SIRT1 may help survival which is linked to the effect on the mitochondrial-apoptotic pathway (35).

Mitochondria are made up of a double membrane system called the outer and inner mitochondrial membranes (MOM and MIM, respectively) (36). The interchange of proteins and lipids between the two membranes is accelerated when they are linked at certain contact locations (37). However, it has been suggested that mitochondrial connection sites are abundant in an anionic phospholipid that results in their unique structure (38). Furthermore, via the permeability transition pore (PTP), a dynamic multi-protein complex found at the interface of the inner and outer mitochondrial membranes (39). Because PTP regulates matrix Ca^{2+} , pH, mitochondrial transmembrane potential, and volume, it plays an important role in metabolic coordination between the cytosol, the mitochondrial intermembrane space, and the matrix (40). The mitochondria consume oxidizing substrates to create an electrochemical proton gradient across the mitochondrial membrane, during a cell's existence, it is utilized to produce ATP. By generating inward transport of cations and outward transport of anions, the direction of the mitochondrial membrane potential promotes cation deposition in the mitochondria. (41). The reactive oxygen species (ROS) induce onset of the MPT which might release soluble mitochondrial factors that activate caspases and initiate apoptosis (40). In this experiment, the use of 5,5,6,6'-tetrachloro-1,1',3,3'-tetraethylbenzimidazolylcarbocyanine iodide (JC-1) dye which has been developed to detect $\Delta\Psi$ in healthy and apoptotic cells, The JC-1 dye is a lipophilic, cationic dye (naturally emitting green fluorescence) that can enter mitochondria, where it accumulates and (concentration-dependently) starts forming reversible complexes called J aggregates that emit excitation and emission in the red spectrum (maximum at 590 nm) rather than green. (42). Figure (7) explains the result in fluorescence microscopy showing high percentage of green for J-monomers to red for J-aggregates when HaCat cells treated with 3mM SNP, JC-1 dye also reaches the mitochondria, which had less negativity due to the increase in membrane permeability, and consequently $\Delta\Psi$ decreases as the process is associated with the attempting to open of the mitochondrial permeability pores and

decline of the electrochemical gradient, as compared to the control group, which can be described as SNP causes apoptosis in HaCat cells, so the JC-1 dye enters the mitochondria, which had less negativity because of increased membrane permeability, and, since JC-1 is cationic dye and under this condition it does not reach a sufficient concentration to trigger the formation of J aggregates thus retaining its original green fluorescence. In The HaCat cell group pretreated with 5 μ M SIRT1 aptamer followed by treatment of 3mM SNP the ratio of green for J-monomers to red for J-aggregates is close to normal (control group) which explain the protective and anti-apoptotic action of SIRT1 aptamer on HaCat cell line by keep mitochondrial function and then mitochondrial membrane potential in a dose-dependent manner. Figure (5 and 6) shows the percentage of apoptotic density of HaCaT cells relative to mitochondrial membrane potential, there is high significant ($p < 0.01$) drop down in $\Delta\Psi$ M at maximum dose of SNP, in other hand there is high significant restoration of $\Delta\Psi$ M compared to control at dose of SIRT1Aptamer (10 μ M) because the activation of SIRT1effectively restored mitochondrial membrane polarization and then anti apoptotic effect. Five μ M SIRT1 aptamer reversed the loss of mitochondria membrane potential, with significant effect at the concentrations with an anti-apoptotic effect. Figure 6 shown that 5 μ M SIRT1 aptamer reversed the loss of MMP, with significant effect at the concentrations with an anti-apoptotic effect.

Mammalian skin has effective antioxidant defense systems that limit oxidative harm to lipids and proteins, hence contributing to barrier integrity, which is necessary for good skin health. As a result, cellular redox balance is required for skin homeostasis, and an imbalance between pro-oxidant and antioxidant pathways can lead to skin illnesses such as aging (43). There is mounting evidence that an increase in ROS levels can affect the activity of the SIRT1 enzyme directly or indirectly. The presence of increased ROS, such as during aging and in various age-related conditions, makes determining the functional role of SIRT1 in these settings difficult (44). This experiment to study the evaluation of the

liberation and accumulation of ROS in HaCat cell line after exposure to SNP and asses the protective activity of SIRT1 aptamer against oxidative stress aging inducer. Figure (8) shown that SIRT1 aptamer produced a dose-dependent drop in percentage of ROS. SIRT1 aptamer at 5 and 10 μ M concentrations significantly decreased ROS level at 1 and 3 mM SNP ($p < 0.01$). Due to a reduction in ROS levels, the DCF fluorescence became steadily lower, accompanied by an increase in SIRT1 aptamer dosage. The results reveal that the SIRT1 aptamer suppresses the interaction of NO with the superoxide anion radical (O_2^-), which produces the extremely lethal ROS peroxynitrite. Degradation of this molecule produces nitrogen dioxide and the radical hydroxyl, which causes DNA damage. (22). So, SIRT1 aptamer can protective the HaCat cell line from peroxynitrite by decreased the ROS level NO overproduction is linked to cellular and tissue damage, neurotoxicity, inflammation, ischemia reperfusion injury, and septic shock. When NO binds directly to a variety of heme centers, including mitochondrial electron transport proteins, it becomes hazardous at higher doses (45). The NO is generated from L-arginine by NO synthases (NOS) (46). Nitric oxygen synthases is divided into two classes, inducible and constitutive. Peroxynitrite is a potent nitrating and oxidizing agent, leading to the nitration of tyrosine residue of target proteins and aberrations of their expression, localization, and function (47,48). NO toxicity in biological systems is primarily caused by the diffusion-limited interaction of NO with to create ($ONOO^-$), which is a highly reactive oxidant that causes lipid peroxidation, thiol oxidation, and nitration of the functional groups of several amino acids including tyrosine (49). Stephan et al, implied that the action of nitric oxide synthase (NOS), triggered by SNP and measured by nitrite accumulation was unaffected by resveratrol which failed to inhibit the production of NO (23, 50). The results in current study counteract the observations in the previous studies using other SIRT1 activator. In figure (10) SIRT1 aptamer at 5 and 10 μ M was significantly attenuate NO ($P < 0.05$) production at the concentrations that protected HaCaT cells against SNP maximal dose (3 mM). Previous study showed that the

early activation of cNOS led to an injury of the cultured cells and skin tissue within 1 h and production of NO (51). SIRT1 aptamer was shown to be able to control the activity of nitric oxide synthase (NOS) triggered by SNP (as evaluated by nitrite accumulation) in the current investigation, demonstrating that its protective impact is linked to NOS suppression. Taken together, this shows that the protective effect of SIRT1 aptamer reported in the current model is due to its ROS scavenging characteristics along with intracellular effector regulation. Apoptosis is a type of planned cell death that is linked to cell death. NO production result in mitochondrial dysfunction and apoptosis (52). Caspase-9 is involved in the execution phase of apoptosis in a variety of ways. Proteolytic cleavage activates caspase-9, which is present as an inactive pro-enzyme. The release of cytochrome c from mitochondria is triggered by ligands of numerous cell surface receptors in a complex linked with the cytoplasmic death domain. Apoptotic protease activation factor 1 binds to cytochrome c, which activates caspase-9, which subsequently cleaves caspase-3 (53). Upstream caspase, such as caspase-9, plays a central role in the induction of apoptosis as a result, determining the intracellular caspase family is critical for understanding the cell apoptosis process (54). However, the increased NO-induced apoptosis by SIRT1 inhibition is mediated by the activation of caspases 3 and 9, but is independent of the caspase 8 pathway (55). Figure (11) shown significantly increased in caspase-9 at SNP dose 3 Mm. In other hands 10 μ M SIRT1 aptamer reduced the increasing activity of caspase-9. This result confirm the previous results in SYTO-16 and JC-1. Moreover, treatment with SIRT1 aptamer led to inhibit a caspase-9 significantly which was increased the cell viability, suggesting that suppressing caspase-9 is an important step in the anti-apoptotic effect generated by SNP. Furthermore, our findings corroborate prior research indicating that SIRT1 inhibits etoposide-induced cell death in HaCaT cells (23).

CONCLUSION

Considering that NO is a key mediator implicated in a broad range of age related skin damages, these findings suggest that SIRT1 aptamer could

delay and prevent the skin aging by blocking apoptotic events and mitochondrial dysfunctions. These data suggest that it could be possible to use SIRT1 aptamer reducing skin aging associated with ROS.

CONFLICTS OF INTEREST

There are no conflicts to declare.

ACKNOWLEDGEMENTS

The authors would like to express their gratitude to College of Pharmacy / Mustansiriyah University (www.uomustansiriyah.edu.iq), Baghdad, Iraq, for its support with this work.

REFERENCES

1. Narendhirakannan R. T., Hannah M. A. Oxidative stress and skin cancer: an overview. *Indian journal of clinical biochemistry*. (2013). *IJCB*, 28(2): 110–115.
2. Cabral-Pacheco GA, Garza-Veloz I, Castruita-De la Rosa C, Ramirez-Acuña JM, Perez-Romero BA, Guerrero-Rodriguez JF, et al. The Roles of Matrix Metalloproteinases and Their Inhibitors in Human Diseases. 2020. Dec 20;21(24):9739.
3. Calapre L., Gray E. S., Kurdykowski S., David, A. Descargues, P., Ziman, M. SIRT1 activation mediates heat-inuced survival of UVB damaged Keratinocytes. *BMC dermatology*. (2017). 17(1): 8.
4. Ming M., Soltani K., Shea C. R., Li, X., & He Y. Y. Dual role of SIRT1 in UVB-induced skin tumorigenesis. *Oncogene*. 2015 Jan 15;34(3):357-63.
5. Al-Sudani B, Ragazzon-Smith AH, Aziz A, Alansari R, Ferry N, Krstic-Demonacos M, Ragazzon PA. Circular and linear: a tale of aptamer selection for the activation of SIRT1 to induce death in cancer cells. *RSC Advances*. 2020;10(73):45008-18.
6. Bielach-Bazyluk A., Zbroch E., Mysliwiec H., Rydzewska-Rosolowska A., Kakareko K., Flisiak I, et al. Sirtuin 1 and skin: implications in intrinsic and extrinsic aging—a systematic review. *Cells*. (2021). 10(4): 813.
7. Al-Sudani BT, Hameed B, Alahmar AT. Gene Expression Analysis in MOTN-1 Cell Line after Treating with New Development Aptamer. *blood cells*. 2020 Feb 1;4:5.
8. Joudah MS, Al-Sudani BT, Arif IS. New Bio-Therapeutic Candidate for Pancreatic Cancer. *Indian Journal of Forensic Medicine & Toxicology*. 2020 Jan 1;14(1).
9. Talib Lj, Al-Abbassi Mg, Al-Sudani BT. Effect

- of SIRT1 Activators on Human Follicular Thyroid Cancer. *International Journal of Pharmaceutical Research*. 2020 Oct;12(4).
10. Qusay A, Marie NK, Al-Sudani BT. Utilization of natural stabilizer to prepare liposomal conjugate for the newly developed aptamer. *Systematic Reviews in Pharmacy*. 2020;11(7):32-50.
 11. TARIQ RA, Al-Sudani BT, Arif IS. Promising Preclinical Data to a Possible Antidiabetic Drug *International Journal of Pharmaceutical Research*, 2020,12 (4).
 12. Joudah MS, Arif IS, Al-Sudani BT. Crosstalk Between Sirt1 Activators And Nf-Kb Axis As A Therapeutic Target To Reduce Pancreatic Cancer. *Systematic Reviews in Pharmacy*. 2021;12(3):207-12.
 13. Al-Sudani BT. Novel therapies for cancer treatment: designing high affinity selective ligands against SIRT1 enzyme. University of Salford (United Kingdom); 2017.
 14. Riss TL, Moravec RA, Niles AL, Duellman S, Benink HA, Worzella TJ, Minor L. Cell viability assays. *Assay Guidance Manual* [Internet]. 2016 Jul 1.
 15. Neri S, Mariani E, Meneghetti A, Cattini L, Facchini A. Calcein-acetyoxymethyl cytotoxicity assay: standardization of a method allowing additional analyses on recovered effector cells and supernatants. *Clinical Diagnostic Laboratory Immunology*. 2001 Nov 1;8(6):1131-5.
 16. Wlodkowic D, Skommer J, Darzynkiewicz Z. Rapid quantification of cell viability and apoptosis in B-cell lymphoma cultures using cyanine SYTO probes. *In Mammalian Cell Viability 2011* (pp. 81-89).
 17. Elefantova K, Lakatos B, Kubickova J, Sulova Z, Breier A. Detection of the mitochondrial membrane potential by the cationic dye JC-1 in L1210 cells with massive overexpression of the plasma membrane ABCB1 drug transporter. *International journal of molecular sciences*. 2018 Jul;19(7):1985.
 18. Lee H, Lee D, Kang KS, Song JH, Choi YK. Inhibition of intracellular ROS accumulation by formononetin attenuates cisplatin-mediated apoptosis in LLC-PK1 cells. *International journal of molecular sciences*. 2018 Mar;19(3):813.
 19. Kumar S, Kashyap P. Antiproliferative activity and nitric oxide production of a methanolic extract of *Fraxinus micrantha* on Michigan Cancer Foundation-7 mammalian breast carcinoma cell line. *Journal of intercultural ethnopharmacology*. 2015 Apr;4(2):109.
 20. El-Huneidi W, Shehab NG, Bajbouj K, Vinod A, El-Serafi A, Shafarin J, Bou Malhab LJ, Abdel-Rahman WM, Abu-Gharbieh E. *Micromeria fruticosa* induces cell cycle arrest and apoptosis in breast and colorectal cancer cells. *Pharmaceuticals*. 2020 Jun;13(6):115.
 21. Weller R. Nitric oxide: a key mediator in cutaneous physiology. *Clin Exp Dermatol*. (2003). 28: 511–514. 1365.
 22. Xia Y, Dawson VL, Dawson TM, Snyder SH, Zweier JL. Nitric oxide synthase generates superoxide and nitric oxide in arginine-depleted cells leading to peroxynitrite-mediated cellular injury. *Proc Natl Acad Sci U S A*. (1996). 93: 6770–6774.
 23. Bastianetto S, Dumont Y, Duranton A, Vercauteren F, Breton L, Quirion R. Protective action of resveratrol in human skin: possible involvement of specific receptor binding sites. *Plos one*. 2010; 5.9: e12935.
 24. Serafeim A, Holder M. J, Grafton G, Chamba A, Drayson M. T, Luong Q. T, et al. Selective serotonin reuptake inhibitors directly signal for apoptosis in biopsy-like Burkitt lymphoma cells. *Blood, The Journal of the American Society of Hematology*. 2003;101.8: 3212-3219.
 25. Bratosin D, Mitrofan L, Paliu C, Estaquier J, Montreuil J. Novel fluorescence assay using calcein-AM for the determination of human erythrocyte viability and aging. *Cytometry Part A: the journal of the International Society for Analytical Cytology*. 2005; 66.1: 78-84.
 26. Probes M. *Molecular SYTO green-fluorescent nucleic acid stains*. Oregon, USA Molecular Probes, Eugene. 2003.
 27. Wlodkowic D, Skommer J, Faley S, Darzynkiewicz Z, Cooper J. M. Dynamic analysis of apoptosis using cyanine SYTO probes: from classical to microfluidic cytometry. *Experimental cell research*. 2009; 315.10: 1706-1714.
 28. Kaštelan M., Prpić-Massari L., Brajac, I. Apoptosis in psoriasis. *Acta Dermatovenerologica Croatica*. (2009); 17(3): 0-0.
 29. Kuranaga, E. Beyond apoptosis: caspase regulatory mechanisms and functions in vivo. *Genes to Cells*. (2012); 17(2): 83-97.
 30. El-Domyati M, Moftah N. H, Nasif G. A., Abdel-Wahab H. M., Barakat, M. T, Abdel-Aziz, R. T. Evaluation of apoptosis regulatory proteins in response to PUVA therapy for psoriasis. *Photodermatology, photoimmunology photomedicine*. (2013); 29(1): 18-26.
 31. Yao X, Hao S, Yu P. Association study of the caspase gene family and psoriasis vulgaris susceptibility in northeastern China. *BioMed research international*. 2019.
 32. Kim, E., Han, S. Y., Hwang, K, Kim, D, Kim, E. M, Hossain, M. A, Cho, J. Y. Antioxidant and cytoprotective effects of (–)-epigallocatechin-3-(3'-o-methyl) gallate. *International journal of molecular sciences*. (2019); 20(16): 3993.
 33. Wlodkowic D, Skommer J, Pelkonen J. Towards an understanding of apoptosis detection by SYTO dyes. *Cytometry Part A: The Journal of the International Society for Analytical Cytology*.

- (2007); 71(2): 61-72.
34. Chung K. W., Choi Y. J., Park M. H., Jang E. J., Kim D. H., Park B. H. Molecular insights into SIRT1 protection against UVB-induced skin fibroblast senescence by suppression of oxidative stress and p53 acetylation. *Journals of Gerontology Series A: Biomedical Sciences and Medical Sciences*, (2015). 70.8; 959:968.
 35. Takayama K, Ishida K, Matsushita T, Fujita N, Hayashi S, Sasaki K, Kuroda R. SIRT1 regulation of apoptosis of human chondrocytes. *Arthritis & Rheumatism*, (2009).60(9); 2731:2740.
 36. Reichert, A. S, Neupert W. Contact sites between the outer and inner membrane of mitochondria—role in protein transport. *Biochimica et Biophysica Acta (BBA)-Molecular Cell Research*. (2002); 1592(1): 41-49.
 37. Horvath S. E., Daum G. Lipids of mitochondria. *Progress in lipid research*. (2013); 52(4): 590-614.
 38. Unsay J. D., Cosentino K, Subburaj Y., García-Sáez A. J. Cardiolipin effects on membrane structure and dynamics. *Langmuir*. (2013); 29(51): 15878-15887.
 39. Bernardi, P. The permeability transition pore. Control points of a cyclosporin A-sensitive mitochondrial channel involved in cell death. *Biochimica et Biophysica Acta (BBA)-Bioenergetics*. (1996); 1275(1-2):5-9.
 40. Zamzami N, Maise C, Métivier D, Kroemer G. Measurement of membrane permeability and the permeability transition of mitochondria. *Methods in cell biology*. (2007); 80: 327-340.
 41. Wlodkowic D, Skommer J, Faley S, Darzynkiewicz Z, Cooper J. M. Dynamic analysis of apoptosis using cyanine SYTO probes: from classical to microfluidic cytometry. *Experimental cell research*. (2009); 315(10): 1706-1714.
 42. Kaštelan M, Prpić-Massari L., Brajac I. Apoptosis in psoriasis. *Acta Dermatovenerologica Croatica*. (2009); 17(3): 0-0.
 43. Briganti S, Picardo, M. Antioxidant activity, lipid peroxidation and skin diseases. What's new. *Journal of the European Academy of Dermatology and Venereology*. (2003);17(6): 663-669.
 44. Kamata H, Honda S. I., Maeda S, Chang L, Hirata H, Karin M. Reactive oxygen species promote TNF α -induced death and sustained JNK activation by inhibiting MAP kinase phosphatases. (2005). 120(5):649-661.
 45. Xia Y., Dawson V. L., Dawson T. M., Snyder S. H., Zweier J. L. Nitric oxide synthase generates superoxide and nitric oxide in arginine-depleted cells leading to peroxynitrite-mediated cellular injury. *Proceedings of the National Academy of Sciences*. (1996); 93(13): 6770-6774.
 46. Kobayashi M, Shu S, Marunaka K, Matsunaga T, Ikari A. Weak ultraviolet B enhances the mislocalization of claudin-1 mediated by nitric oxide and peroxynitrite production in human keratinocyte-derived HaCaT cells. *International journal of molecular sciences*. 2020 Jan;21(19):7138.
 47. Tejero J, Shiva S, Gladwin M. T. Sources of vascular nitric oxide and reactive oxygen species and their regulation. *Physiological reviews*. (2019); 99(1): 311-379.
 48. Cals-Grierson M. M, Ormerod A. D. Nitric oxide function in the skin. *Nitric oxide*. (2004);10(4): 179-193.
 49. Dawson V. L., Dawson T. M., London E. D., Bredt, D. S., Snyder S. H. Nitric oxide mediates glutamate neurotoxicity in primary cortical cultures. *Proceedings of the National Academy of sciences*. (1991); 88(14): 6368-6371.
 50. Bastianetto S., Zheng W. H., Quirion, R. Neuroprotective abilities of resveratrol and other red wine constituents against nitric oxide-related toxicity in cultured hippocampal neurons. *British journal of pharmacology*. (2000); 131(4): 711-720.
 51. Wu S., Wang L., Jacoby A. M., Jasinski K., Kubant R., Malinski, T. Ultraviolet B Light-induced Nitric Oxide/Peroxynitrite Imbalance in Keratinocytes—Implications for Apoptosis and Necrosis. *Photochemistry and photobiology*. (2010); 86(2): 389-396.
 52. Pérez-Matute P., Zulet M. A., Martínez J. A. Reactive species and diabetes: counteracting oxidative stress to improve health. *Current opinion in pharmacology*. (2009); 9(6): 771-779.
 53. Zhang L., Lei J., Liu J., Ma F., Ju H. In situ activation and monitoring of the evolution of the intracellular caspase family. *Chemical science*. (2015); 6(6): 3365-3372.
 54. Takayama K., Ishida K., Matsushita T., Fujita N., Hayashi S, Sasaki K, Kuroda, R. SIRT1 regulation of apoptosis of human chondrocytes. *Arthritis & Rheumatism*. (2009); 60(9): 2731-2740.
 55. Wu Y., Zhao D., Zhuang, J., Zhang F., Xu C. Caspase-8 and caspase-9 functioned differently at different stages of the cyclic stretch-induced apoptosis in human periodontal ligament cells. *PLoS One*. (2016);11(12): e0168268.